GLOBAL BIOGEOCHEMICAL CYCLES, VOL. 12, NO. 2, PAGES 213–230, JUNE 1998

Testing global ocean carbon cycle models using measurements of atmospheric O_2 and CO_2 concentration

Britton B. Stephens,[1] Ralph F. Keeling,[1] Martin Heimann,[2] Katharina D. Six,[2] Richard Murnane,[3] and Ken Caldeira[4]

Abstract. We present a method for testing the performance of global ocean carbon cycle models using measurements of atmospheric O_2 and CO_2 concentration. We combine these measurements to define a tracer, atmospheric potential oxygen (APO $\approx O_2 + CO_2$), which is conservative with respect to terrestrial photosynthesis and respiration. We then compare observations of APO to the simulations of an atmospheric transport model which uses ocean-model air-sea fluxes and fossil fuel combustion estimates as lower boundary conditions. We present observations of the annual-average concentrations of CO_2, O_2, and APO at 10 stations in a north-south transect. The observations of APO show a significant interhemispheric gradient decreasing towards the north. We use air-sea CO_2, O_2, and N_2 fluxes from the Princeton ocean biogeochemistry model, the Hamburg model of the ocean carbon cycle, and the Lawrence Livermore ocean biogeochemistry model to drive the TM2 atmospheric transport model. The latitudinal variations in annual-average APO predicted by the combined models are distinctly different from the observations. All three models significantly underestimate the interhemispheric difference in APO, suggesting that they underestimate the net southward transport of the sum of O_2 and CO_2 in the oceans. Uncertainties in the model-observation comparisons include uncertainties associated with the atmospheric measurements, the atmospheric transport model, and the physical and biological components of the ocean models. Potential deficiencies in the physical components of the ocean models, which have previously been suggested as causes for anomalously large heat fluxes out of the Southern Ocean, may contribute to the discrepancies with the APO observations. These deficiencies include the inadequate parameterization of subgrid-scale isopycnal eddy mixing, a lack of subgrid-scale vertical convection, too much Antarctic sea-ice formation, and an overestimation of vertical diffusivities in the main thermocline.

1. Introduction

Global ocean carbon cycle models, consisting of ocean general circulation models with biological parameterizations or submodels, are becoming valuable tools for investigating and quantifying organic matter cycling, new production, and the uptake of anthropogenic CO_2 on regional and global scales [*Sarmiento et al.*, 1995; *Six and Maier-Reimer*, 1996]. Initial comparisons between such models and observations, which indicated an unrealistic buildup of nutrients in the equatorial region, contributed to an increased awareness of the importance of dissolved organic carbon (DOC) in nutrient transport [*Sarmiento et al.*, 1988; *Bacastow and Maier-Reimer*, 1991; *Najjar et al.*, 1992]. These models have also produced significantly increased estimates of global new production, of the order of 10 Gt C yr^{-1} [*Sarmiento et al.*, 1993; *Six and Maier-Reimer*, 1996]. Ocean carbon cycle models have recently been applied toward estimating how much anthropogenic CO_2 has been taken up by the oceans [*Sarmiento et al.*, 1995, *Heimann and Maier-Reimer*, 1996] and predicting how climate change might affect future uptake [*Sarmiento and Le Quéré*, 1996; *Maier-Reimer et al.*, 1996].

The regional predictions of global carbon cycle models have a bearing on a controversy involving the relative importance of the northern terrestrial biota and the northern hemisphere oceans, particularly the North Atlantic, in absorbing anthropogenic CO_2 [*Keeling et al.*, 1989b; *Tans et al.*, 1990]. The atmospheric CO_2 and $^{13}CO_2/^{12}CO_2$ measurements of *Keeling et al.* [1989b], when compared to results from an atmospheric transport model, indicated a 1 Gt C yr^{-1} sink in the North Atlantic Ocean. However, *Tans et al.* [1990], also using an atmospheric transport model, found that surface pCO_2 measurements were inconsistent with such a sink and concluded that a large sink in northern terrestrial biota was required to explain the interhemispheric CO_2 gradient. More recently, the ocean carbon cycle model of *Sarmiento et al.* [1995] predicted that the Atlantic Ocean north of 18°S is currently taking up 0.4 Gt C yr^{-1}, which by subtraction implies a relatively large northern terrestrial CO_2 sink. The surface pCO_2 values in this model were in good agreement with the

[1]Scripps Institution of Oceanography, University of California, San Diego, La Jolla.
[2]Max Planck Institut für Meteorologie, Hamburg, Germany.
[3]Bermuda Biological Station for Research, Inc., Ferry Reach, St. George's, Bermuda.
[4]Lawrence Livermore National Laboratory, Livermore, California.

Paper number 97GB03500.
0886-6236/98/97GB-03500$12.00

measurements of *Takahashi et al.* [1995]. However, as *Sarmiento et al.* [1995] discussed, the balance between the implied atmospheric CO_2 sink, riverine inputs, and the observed southward transport of dissolved inorganic carbon (DIC) in the Atlantic [*Brewer et al.*, 1989; *Broecker and Peng*, 1992] is not well understood.

We have examined output from three models, the Princeton ocean biogeochemistry model (POBM) [*Sarmiento et al.*, 1995; *Najjar*, 1990], the Hamburg model of the ocean carbon cycle (HAMOCC3.1) [*Six and Maier-Reimer*, 1996; *Maier-Reimer*, 1993], and the Lawrence Livermore ocean biogeochemistry model (LLOBM) (K. Caldeira et al., manuscript in preparation, 1998), in this study. Because these models are under active development and because of their wide reaching and often unique predictions, there is a strong need to test these models against observed data sets. These models have been extensively compared to observed ocean nutrient and tracer distributions [*Bacastow and Maier-Reimer*, 1991; *Najjar et al.*, 1992; *Gruber et al.*, 1996; K. Caldeira et al., manuscript in preparation, 1998]. Although the biological parameterizations are highly simplified and the physical models are relatively coarse, the model predictions are in qualitative agreement with oceanic nutrient and tracer data such as ^{14}C [*Toggweiler et al.*, 1989a, b], PO_4 [*Anderson and Sarmiento*, 1995; *Six and Maier-Reimer*, 1996], and apparent oxygen utilization [*Anderson and Sarmiento*, 1995]. Resolving the quantitative discrepancies with these data, however, will not necessarily improve the representation of air-sea fluxes. If there are any errors in the hydrographic transports, optimizing the models to match oceanic observations would actually produce errors in air-sea exchange. Thus a sensitive validation of these models also requires a means of testing the predicted air-sea fluxes themselves.

Our approach to testing these air-sea fluxes is to compare the variations they produce in an atmospheric transport model to observations of a composite tracer approximately equal to the sum of atmospheric O_2 and CO_2. In an ideal world in which atmospheric carbon existed only as CO_2 and modern and fossil terrestrial carbon existed only as CH_2O, the sum of atmospheric CO_2 and O_2 would be conservative with respect to terrestrial photosynthesis, respiration, and fossil fuel combustion and only sensitive to air-sea exchange [*Keeling and Shertz*, 1992; *Keeling et al.*, 1998b]. Thus observations of the sum of CO_2 and O_2 can be used to test atmosphere-ocean model predictions irrespective of terrestrial CO_2 and O_2 exchange. We refer to this sum, which is effectively the amount of O_2 that would be left in an air parcel after all of its CO_2 was reduced through photosynthesis, as atmospheric potential oxygen (APO). We present a more explicit definition of APO below, in which we account for complexities due to variations in the reduction of nitrogen and other species during photosynthesis and to the oxidation of CO and CH_4 in the atmosphere.

Six and Maier-Reimer [1996] recently presented a favorable comparison between the results of an atmospheric transport model driven by HAMOCC3.1 O_2 fluxes and seasonal observations of atmospheric O_2 at Cape Grim, Tasmania. Here we emphasize primarily the test of the nonseasonal component of the modeled atmospheric concentrations. We find large discrepancies between the observed latitudinal APO gradients and those predicted by all three ocean models. This result may be consistent with postulated problems in the models' hydrographic tracer transports. These comparisons represent a method for independently testing the models' representations of physical and biological processes and a means to target aspects of the models which may require future improvement. Because the biogeochemical controls on APO are somewhat more complicated than for CO_2 or O_2 alone, we will briefly discuss the relevant oceanic processes before presenting the model-observation comparison.

2. Ocean Biogeochemical Controls on CO_2 and O_2

The regional fluxes of CO_2 and O_2 across the air-sea interface are driven by three distinct processes: (1) temperature- and salinity-related solubility effects known as the solubility pump, (2) biological production and respiration known as the biological pump, and (3) atmospheric buildup of anthropogenic CO_2. Where waters near the surface are warmed, such as at low latitudes in association with equatorial upwelling, the decreasing solubilities lead to net effluxes of CO_2 and O_2 into the atmosphere. Conversely, where waters near the surface are cooled, for example, at high latitudes or in association with poleward current systems such as the Gulf Stream, increasing solubilities lead to net CO_2 and O_2 influx. Because salinity influences are relatively small, air-sea fluxes due to the solubility pump are primarily the result of temperature changes closely associated with air-sea heat fluxes. These thermally driven CO_2 and O_2 fluxes are superimposed on biologically driven fluxes that are closely associated with changes in preformed nutrients [*Keeling et al.*, 1993]. Along the equator and at high latitudes, the supply of DIC, O_2 deficit, and nutrients to the surface exceeds the rate of local productivity, leading to net CO_2 efflux, net O_2 influx, and the creation of preformed nutrients. Conversely, as these waters spread laterally into the subtropical gyres and their preformed nutrients are consumed, they take up CO_2 and give off O_2.

The effects of the solubility and biological pumps on air-sea CO_2 fluxes have been discussed extensively [*Volk and Hoffert*, 1985; *Sarmiento et al.*, 1995]. The interaction of these processes is somewhat different for O_2. In high-latitude regions, where DIC rich, O_2-depleted waters are brought to the surface and cooled, the biological and solubility pumps have opposing effects on air-sea CO_2 fluxes but have reinforcing effects on O_2 fluxes. In the equatorial upwelling zones, the effects of the solubility and biological pumps on air-sea exchange tend to reinforce for CO_2 and counteract for O_2 because of the warming of the upwelled water. However, as this water spreads laterally and nutrients are depleted through photosynthesis, the two pumps tend to reinforce for O_2 and counteract for CO_2 over the broader equatorial region. The reinforcing tendency of the solubility and biological pumps on the large-scale air-sea O_2 exchanges, which occurs over most of the ocean surface, makes atmospheric O_2 particularly sensitive to large-scale patterns of ocean circulation.

The effects of the solubility and biological pumps on air-sea APO fluxes will be a complex combination of their effects on O_2 and CO_2 individually. Because the solubility pump affects air-sea CO_2 and O_2 fluxes in the same direction, it will

Table 1. Sampling Stations in the Scripps O_2/N_2 Network

Station Code	Site	Latitude	Longitude	Elevation, m	Time Period
ALT	Alert, Northwest Territories	82°27'N	62°31'W	210	Nov. to Dec. 1989 April 1991 to Oct. 1996
CBA	Cold Bay, Alaska	55°12'N	162°43'W	25	Aug. 1995 to Nov. 1996
NWR	Niwot Ridge, Colorado	40°03'N	105°38'W	3749	April 1991 to April 1993
LJO	La Jolla, California	32°52'N	117°15'W	20	May 1989 to Oct. 1996
	Mauna Loa, Hawaii	19°32'N	155°35'W	3397	Aug. 1993 to Nov. 1996
KUM	Kumukahi, Hawaii	19°31'N	154°49'W	40	June 1993 to Oct. 1996
SMO	Cape Matatula, American Samoa	14°15'S	170°34'W	42	June 1993 to Oct. 1996
	Cape Grim, Tasmania	40°41'S	144°41'E	94	Jan. 1991 to Oct. 1996
	Macquarie Island	54°29'S	158°58'E	94	Sept. 1992 to Jan. 1994
SPO	South Pole Station	89°59'S	24°48'W	2810	Nov. 1991 to Feb. 1996

have a strong effect on APO in the sense of outgassing at low latitudes where the oceans are warmed and ingassing in high-latitude regions where the ocean is cooled. Because the biological pump affects CO_2 and O_2 in opposite directions, it will have a weaker effect on APO. We do not expect the biological CO_2 and O_2 fluxes to perfectly cancel, however, because of the reduction of nitrogen during marine photosynthesis, alkalinity changes which affect CO_2 but not O_2, and differences between the rates of CO_2 and O_2 gas exchange. The greater influence of the solubility pump on APO fluxes implies that variations in APO will be particularly sensitive to oceanic heat fluxes.

3. Observations and Fossil Fuel Predictions

We have measured CO_2 and O_2 concentrations in air which was collected in flasks approximately biweekly at a global network of 10 stations as shown in Table 1 and Figure 1. We measure CO_2 using a nondispersive infrared analyzer and O_2 by an interferometric technique [*Keeling*, 1988, *Keeling et al.*, 1998a]. We report O_2 concentrations as changes in O_2/N_2 ratio. We fit the observed records at each station with the sum of a stiff-spline interannual trend and a four-harmonic seasonal cycle. Owing to the shortness of the records at Cold Bay, Niwot Ridge, and Macquarie Island, we use fixed trends

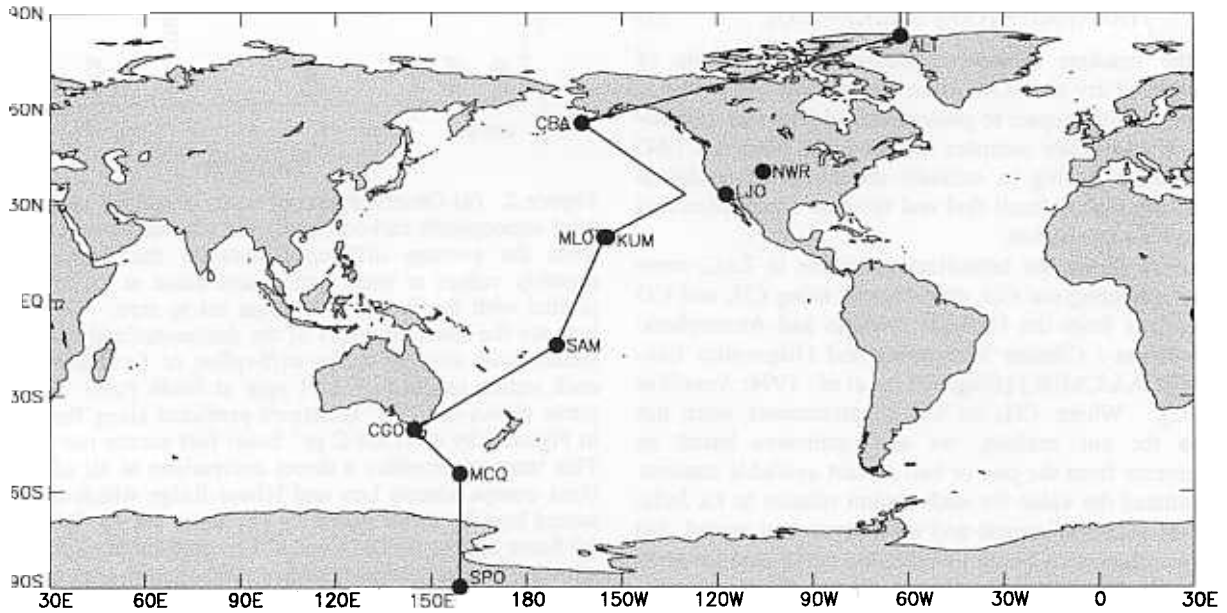

Figure 1. Showing the locations of the stations in the Scripps O_2/N_2 sampling network as listed in Table 1. The solid line indicates the surface transect used to present the model predictions in Figures 2-6.

and a two-harmonic fit at these stations. For seasonal cycle comparisons, we look only at the harmonic fits. To derive relative concentration or ratio differences between stations, we first adjust each observed value to the 15th of its month by sliding it parallel to the combined stiff-spline and harmonic fit. We then average the observations for each month and subtract the harmonic fit from these monthly values to deseasonalize the data. We compute relative CO_2 and O_2/N_2 differences between stations by averaging the differences between these deseasonalized monthly values over the period of overlapping observations. Although we observe meaningful interannual variations in these relative differences [*Keeling et al.*, 1996], our focus here is on the averages of the differences over the several years of observation, as we are comparing to models with no interannual variations. We do not have long enough records to calculate meaningful estimates of the uncertainty in our comparisons due to natural interannual variability. Although more observations are needed to characterize the stability of the observed patterns over longer time frames, the dominant patterns presented here were stable over the periods shown in Table 1.

3.1. CO_2 Gradients

As *Enting and Mansbridge* [1989] point out, the relationship between atmospheric concentrations and surface sources of CO_2 is sensitive to the photochemical oxidation of CO to CO_2 and CH_4 to CO in the atmosphere. This same sensitivity applies to O_2. Recent studies [*Enting et al.*, 1995; *Erickson et al.*, 1996] have attempted to estimate the relative CO contributions from incomplete combustion of fossil fuels and biomass and the oxidation of CH_4, in order to correct their model CO_2 concentrations so that they could be directly compared to observations. Instead of correcting our model values, we correct our observations, using observed CH_4 and CO concentrations. To correct our CO_2 observations, we compute total atmospheric carbon (TAC) as

$$\text{TAC (ppm)} = [CO_2] + [CH_4] + [CO] \quad (1)$$

where the brackets indicate a measurement in units of μmole/mole of dry air. TAC is an atmospheric tracer that is conservative with respect to photochemical CH_4 and CO oxidation. We can then compare modeled and observed TAC values without having to estimate the extent of oxidation which occurs during fossil fuel and biomass combustion and organic matter respiration.

Figure 2a shows the latitudinal variations in TAC, computed by correcting our CO_2 observations using CH_4 and CO measurements from the National Oceanic and Atmospheric Administration / Climate Monitoring and Diagnostics Laboratory (NOAA/CMDL) [*Dlugokencky et al.*, 1994; *Novelli et al.*, 1992]. Where CH_4 or CO measurements were not available for our stations, we used estimates based on measurements from the one or two closest available stations. We calculated the value for each station relative to La Jolla, the station with the longest and most consistent record, but plot these values with South Pole Station set to zero for visualization purposes. The error bars in Figure 2a represent the standard errors of the deseasonalized monthly residuals with respect to the stiff-spline or fixed-trend fits. This error accounts for measurement imprecision and synoptic variability in the observed differences but not for interannual variability which is taken up by the stiff spline. Because of CO_2 sampling problems at Macquarie Island, we have assumed that its CO_2 value is 0.0 ± 0.5 ppm relative to Cape Grim (R. Francey, personal communication, 1996). These observations define a relatively smooth northward increasing gradient, as we expect due to fossil fuel burning.

We also show in Figure 2a the TAC variations relative to South Pole Station predicted by forcing the TM2 atmospheric transport model (described below) with a 6.1 Gt C yr^{-1} fossil fuel source [*Marland et al.*, 1985; *Andres et al.*, 1998]. We interpolate the atmospheric model results along a surface transect as shown in Figure 1. We compare the La Jolla observations to model predictions one gridbox to the west, because the TM2 gridbox which contains La Jolla has strong fossil fuel sources, whereas the sampling times at this station

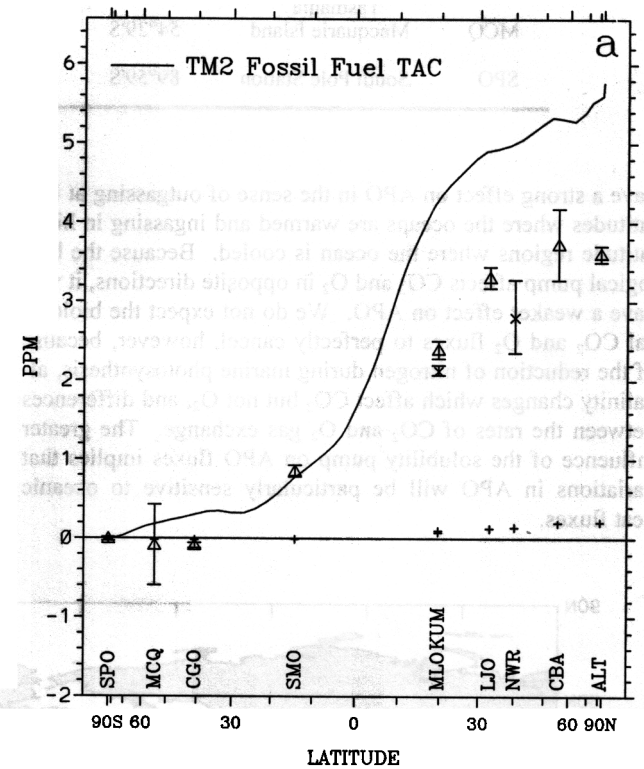

Figure 2. (a) Observed annual mean latitudinal variations in total atmospheric carbon (TAC) (Δ). Values were calculated from the average difference between the deseasonalized monthly values at each station and those at La Jolla, then plotted with the South Pole value set to zero. The vertical bars are the standard errors of the deseasonalized monthly residuals with respect to the stiff-spline or fixed trend fits at each station (equal to ± 0.01 ppm at South Pole). The solid curve shows the TAC variations predicted along the transect in Figure 1 by a 6.1 Gt C yr^{-1} fossil fuel source run on TM2. This transect provides a direct comparison at all of the stations except Mauna Loa and Niwot Ridge which are represented here by cross symbols. (b) Same but for $\delta(O_2/N_2)_{corr}$. (c) Same but for APO. Vertical bars include the influence of allowing the terrestrial oxidative ratio to vary over the range 1.1 ± 0.05. The plus symbols in Figures 2a, 2b, and 2c represent the combined contribution of the CO and CH_4 terms in Equations (1), (3), and (4), respectively. The vertical axes have been scaled so that Figure 2c is graphically the sum of Figures 2a and 2b.

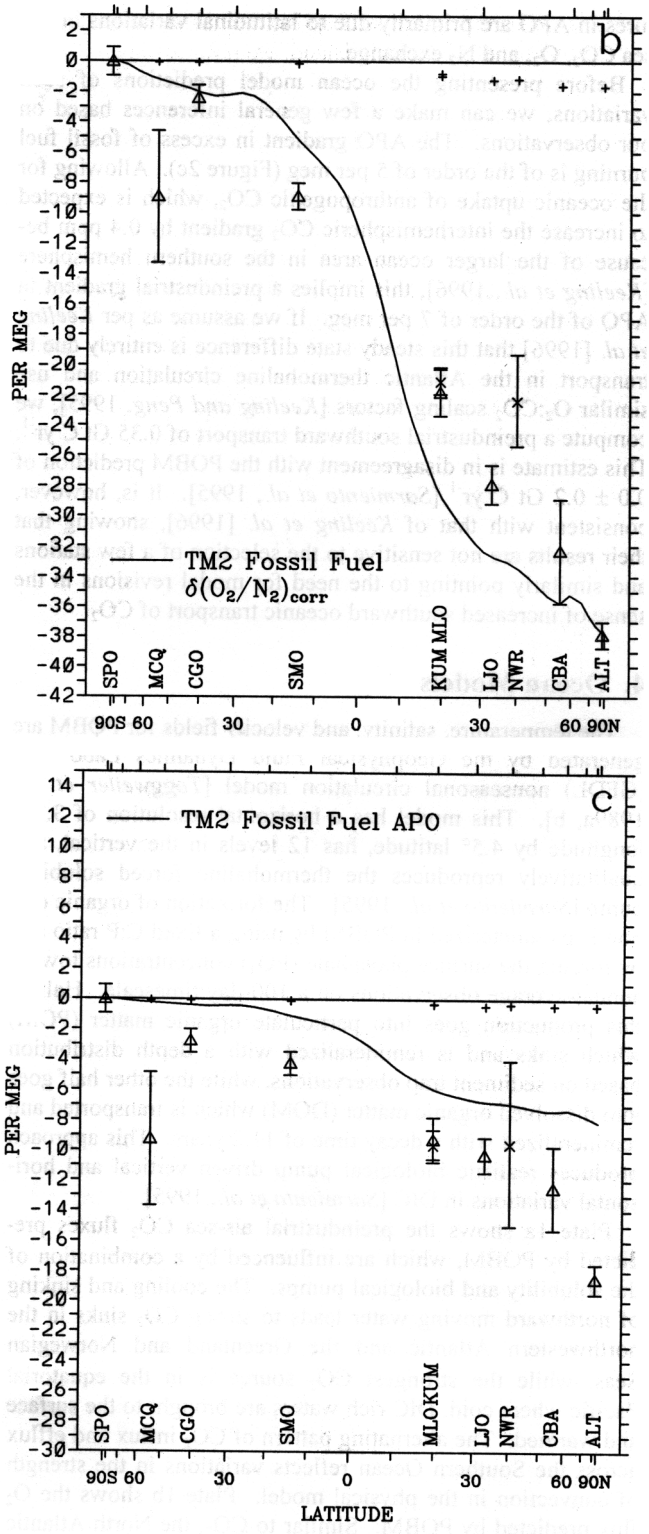

Figure 2. (continued)

are selected to coincide with wind conditions that deliver clean marine boundary layer air. This surface transect thus allows direct comparisons at all stations except for Mauna Loa and Niwot Ridge. For TAC, this comparison shows (Figure 2a) a significant discrepancy between the modeled and observed gradients which has previously been used to infer that a large unaccounted CO_2 sink must exist in the northern hemisphere [*Keeling et al.*, 1989b; *Tans et al.*, 1990].

3.2. O_2 Gradients

We express differences in O_2/N_2 ratio in "per meg" units according to

$$\delta(O_2/N_2) = [(O_2/N_2)_{sample}/(O_2/N_2)_{reference} - 1] \times 10^6. \quad (2)$$

We have accounted for the interference effects of CO_2, CH_4, and CO on our interferometric O_2 measurements using concurrent CO_2 measurements and NOAA/CMDL CH_4 and CO values [*Dlugokencky et al.*, 1994; *Novelli et al.*, 1992]. To correct our O_2 observations for the influence of photochemical CH_4 and CO oxidation, we define corrected O_2/N_2 as

$$\delta(O_2/N_2)_{corr}\ (\text{per meg}) = \delta(O_2/N_2) - (2.0/X_{O2})[CH_4] - (0.5/X_{O2})[CO] \quad (3)$$

where the O_2 mole fraction (X_{O2} = 0.2095) is needed to convert from "ppm" to "per meg" units [*Keeling et al.*, 1998a]. Ignoring the relatively small absolute variations in other molecules that undergo photochemical oxidation, reduction, or heterogeneous loss, the tracer $\delta(O_2/N_2)_{corr}$ represents the atmospheric O_2/N_2 that one would measure after CH_4 and CO were both fully oxidized.

Figure 2b shows the observed latitudinal variations in $\delta(O_2/N_2)_{corr}$ along with the fossil fuel predictions. These fossil fuel predictions account for the different oxidative ratios and spatial distributions of gas, liquid, and solid fuel combustion, gas-flaring, and cement manufacture [*Marland et al.*, 1985; *Keeling*, 1988; *Andres et al.*, 1998]. To obtain the annual mean value from the limited observations at Macquarie Island, we compared the observations to the fitted curve for Cape Grim and computed the Macquarie Island - Cape Grim difference. The relatively large error bars for Macquarie Island result from the inclusion or exclusion of several possible outliers. The $\delta(O_2/N_2)_{corr}$ value at Niwot Ridge may be anomalously high, and the TAC value may be low, because of the influence of local vegetation on daytime samples.

The interhemispheric $\delta(O_2/N_2)_{corr}$ gradient decreases toward the northern hemisphere, as we would expect from fossil fuel combustion. However, similarly to the TAC case and as shown previously by *Keeling et al.* [1996], the fossil fuel source run on TM2 overpredicts the difference in $\delta(O_2/N_2)_{corr}$ between northern and southern midlatitudes. It is clear that terrestrial and oceanic exchanges of CO_2, O_2, and N_2 must also be affecting the latitudinal variations of these species.

3.3. Derivation of Atmospheric Potential Oxygen

Because the relationships between air-sea CO_2 and O_2 exchanges are complex, it is not possible to use atmospheric CO_2 and O_2 measurements alone to separate the terrestrial and oceanic components of the observed latitudinal variations unless other constraints on the air-sea fluxes are invoked [e.g., *Keeling et al.*, 1996]. However, if we had a global ocean carbon cycle model that could predict the oceanic component of the atmospheric variations, we could determine the terrestrial CO_2 and O_2 components by subtraction, and furthermore we would expect these CO_2 and O_2 components to be stoichiometrically consistent with terrestrial processes. Here we instead reverse this concept by combining the TAC and

$\delta(O_2/N_2)_{corr}$ measurements to eliminate any terrestrial influences and checking to see if the results are consistent with ocean model predictions.

To do this, we define atmospheric potential oxygen as

$$\begin{aligned} \text{APO (per meg)} &= \delta(O_2/N_2)_{corr} + (1.1/X_{O2})\text{TAC} \\ &= \delta(O_2/N_2) + (1.1/X_{O2})[CO_2] \\ &\quad - (0.9/X_{O2})[CH_4] + (0.6/X_{O2})[CO] \end{aligned} \tag{4}$$

where X_{O2} again converts from "ppm" to "per meg" units and the factor of 1.1 represents the O_2:CO_2 exchange ratio for terrestrial photosynthesis and respiration as determined by Severinghaus [1995]. This value, which exceeds unity because of the reduction and oxidation of nitrogen and other elements, was estimated based on an analysis of elemental abundances and direct measurements [*Severinghaus*, 1995; *Keeling*, 1988]. The tracer APO represents the atmospheric O_2/N_2 ratio one would measure if all CH_4 and CO molecules were oxidized to CO_2 and then all CO_2 was converted to O_2 through terrestrial photosynthesis (comparable to "Oceanic O_2/N_2" of *Keeling and Shertz* [1992] and Keeling *et al.* [1998b]). This tracer is thus conservative with respect to the oxidation of CH_4 and CO and with respect to terrestrial exchange. Variations in APO can be caused only by air-sea exchange of CO_2, O_2, and N_2 and a fossil fuel effect resulting from the higher O_2:C oxidative ratios for fossil fuels than for terrestrial organic matter.

To model changes in APO in an air parcel due to changes in the number of moles of an individual species (e.g., ΔO_2, ΔN_2, and ΔCO_2), we can write

$$\begin{aligned} \Delta\text{APO} &= (\partial\text{APO}/\partial O_2)\Delta O_2 + (\partial\text{APO}/\partial N_2)\Delta N_2 \\ &\quad + (\partial\text{APO}/\partial CO_2)\Delta CO_2 \\ &= [(1.0/X_{O2})\Delta O_2 - (1.0/X_{N2})\Delta N_2 \\ &\quad + (1.1/X_{O2})\Delta CO_2]/M \end{aligned} \tag{5}$$

where M represents the initial number of moles in the air parcel and X_{N2}, the N_2 mole fraction, is equal to 0.7808. Figure 2c shows the observed latitudinal variations in APO, along with those predicted for the fossil fuel effect, where the fossil fuel effect is calculated according to the first and last terms in (5). The observed error bars here represent a quadrature sum of the statistical error and the variation produced by allowing the terrestrial oxidative ratio to vary over the range 1.1 ± 0.05 per *Severinghaus* [1995]. Figure 2 also indicates that the CH_4 and CO photochemical correction terms sum to approximately 5% of the TAC and $\delta(O_2/N_2)_{corr}$ signals but that their contributions are less significant to APO.

With local terrestrial influences removed, the APO value at Niwot Ridge is closer to the values for La Jolla and Cold Bay. Fossil fuel combustion has a significant effect on APO because of the higher oxidative ratio in fossil fuels, of around 1.4, relative to terrestrial biotic matter. However, the predicted fossil fuel effect on APO does not account for the Cold Bay - Alert difference, the South Pole - Cape Grim difference, nor the Macquarie Island depression. We expect these features in APO are primarily due to latitudinal variations in air-sea CO_2, O_2, and N_2 exchange.

Before presenting the ocean model predictions of such variations, we can make a few general inferences based on our observations. The APO gradient in excess of fossil fuel burning is of the order of 5 per meg (Figure 2c). Allowing for the oceanic uptake of anthropogenic CO_2, which is expected to increase the interhemispheric CO_2 gradient by 0.4 ppm because of the larger ocean area in the southern hemisphere [*Keeling et al.*, 1996], this implies a preindustrial gradient in APO of the order of 7 per meg. If we assume as per *Keeling et al.* [1996] that this steady state difference is entirely due to transport in the Atlantic thermohaline circulation and use similar O_2:CO_2 scaling factors [*Keeling and Peng*, 1995], we compute a preindustrial southward transport of 0.35 Gt C yr^{-1}. This estimate is in disagreement with the POBM prediction of 0.0 ± 0.2 Gt C yr^{-1} [*Sarmiento et al.*, 1995]. It is, however, consistent with that of *Keeling et al.* [1996], showing that their results are not sensitive to the selection of a few stations and similarly pointing to the need for model revisions in the sense of increased southward oceanic transport of CO_2.

4. Ocean Models

The temperature, salinity, and velocity fields for POBM are generated by the Geophysical Fluid Dynamics Laboratory (GFDL) nonseasonal circulation model [*Toggweiler et al.*, 1989a, b]. This model has a horizontal resolution of 3.75° longitude by 4.5° latitude, has 12 levels in the vertical, and qualitatively reproduces the thermohaline forced solubility pump [*Sarmiento et al.*, 1995]. The formation of organic carbon is parameterized in POBM by using a fixed C:P ratio and by forcing the surface phosphate (PO_4) concentrations toward annual-average observations on a 100-day timescale. Half of this production goes into particulate organic matter (POM) which sinks and is remineralized with a depth distribution based on sediment trap observations, while the other half goes into dissolved organic matter (DOM) which is transported and remineralized with a decay time of 11.2 years. This approach produces realistic biological pump driven vertical and horizontal variations in DIC [*Sarmiento et al.*, 1995].

Plate 1a shows the preindustrial air-sea CO_2 fluxes predicted by POBM, which are influenced by a combination of the solubility and biological pumps. The cooling and sinking of northward moving water leads to strong CO_2 sinks in the northwestern Atlantic and the Greenland and Norwegian Seas, while the strongest CO_2 source is in the equatorial Pacific where cold, DIC rich waters are brought to the surface and warmed. The alternating pattern of CO_2 influx and efflux across the Southern Ocean reflects variations in the strength of convection in the physical model. Plate 1b shows the O_2 flux predicted by POBM. Similar to CO_2, the North Atlantic regions of deep water formation are sinks for O_2. In the equatorial Pacific, the biological depletion of O_2 in the upwelling waters produces a sink along the equator. However, as these nutrient rich waters spread outward from the equator, enhanced new production and warming lead to a net source of O_2 for the equatorial region. The strong Southern Ocean O_2 sinks appear to correspond to regions of CO_2 efflux, indicat-

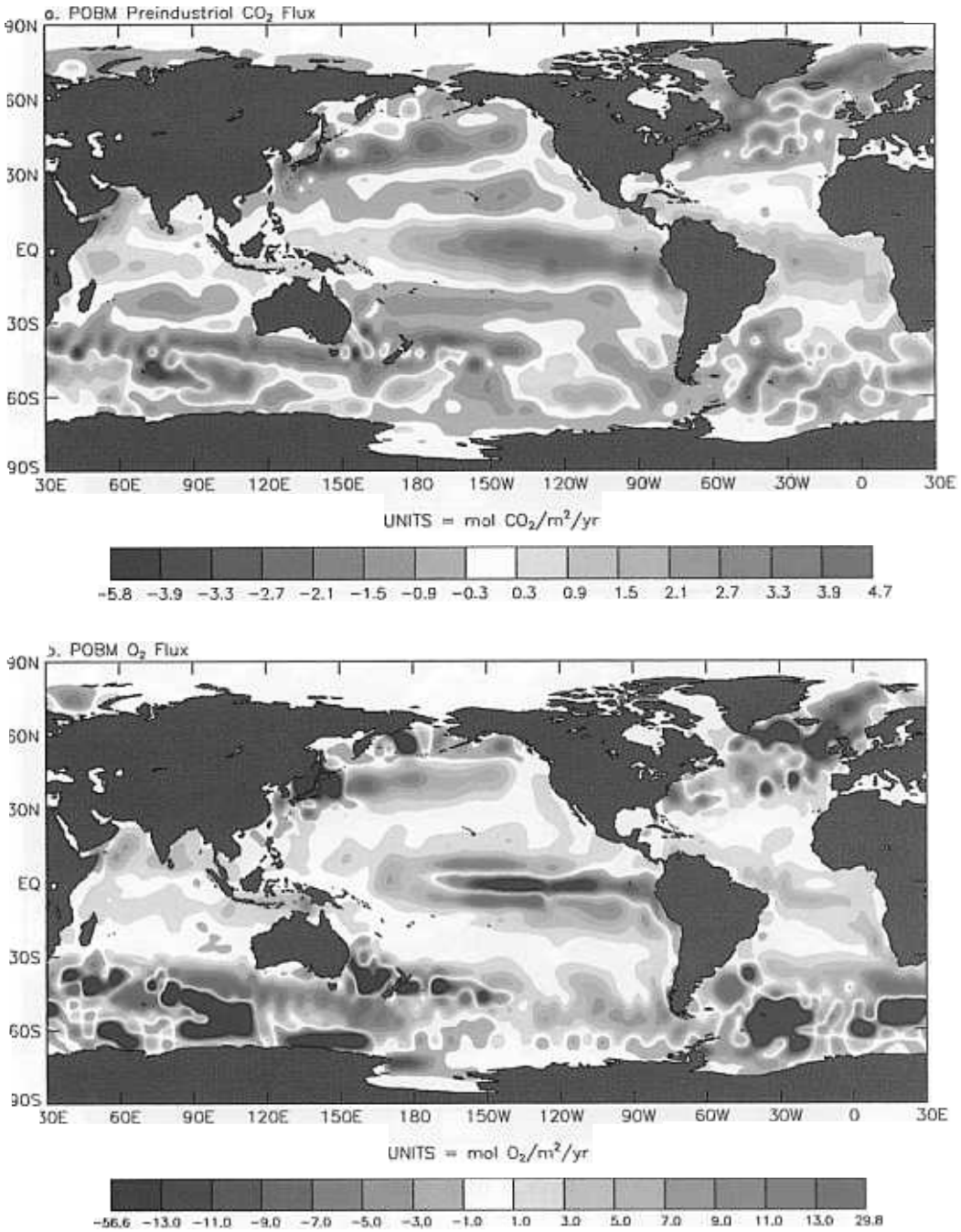

Plate 1. (a) The preindustrial sea-air CO_2 flux in mol CO_2 m^{-2} yr^{-1} as predicted by the Princeton ocean biogeochemistry model (POBM). The grid spacing of these fluxes is 3.75° longitude by 4.5° latitude. (b) Same but for sea-air O_2 flux in mol O_2 m^{-2} yr^{-1}. (c) Same as Plate 1a but as predicted by the Hamburg model of the ocean carbon cycle (HAMOCC3.1). The original 3.5° by 3.5° diagonal grid was interpolated onto a 2.5° by 2.5° rectangular grid before contouring. (d) Same as Plate 1b but as predicted by HAMOCC3.1. (e) Same as Plate 1a but as predicted by the Lawrence Livermore ocean biogeochemistry model (LLOBM). These fluxes have a resolution of 4° longitude by 2° latitude. (f) Same as Plate 1b but as predicted by LLOBM. Note the similar contour levels, with the exception of the extreme values, between Plates 1a, 1c, and 1e, and between Plates 1b, 1d, and 1f.

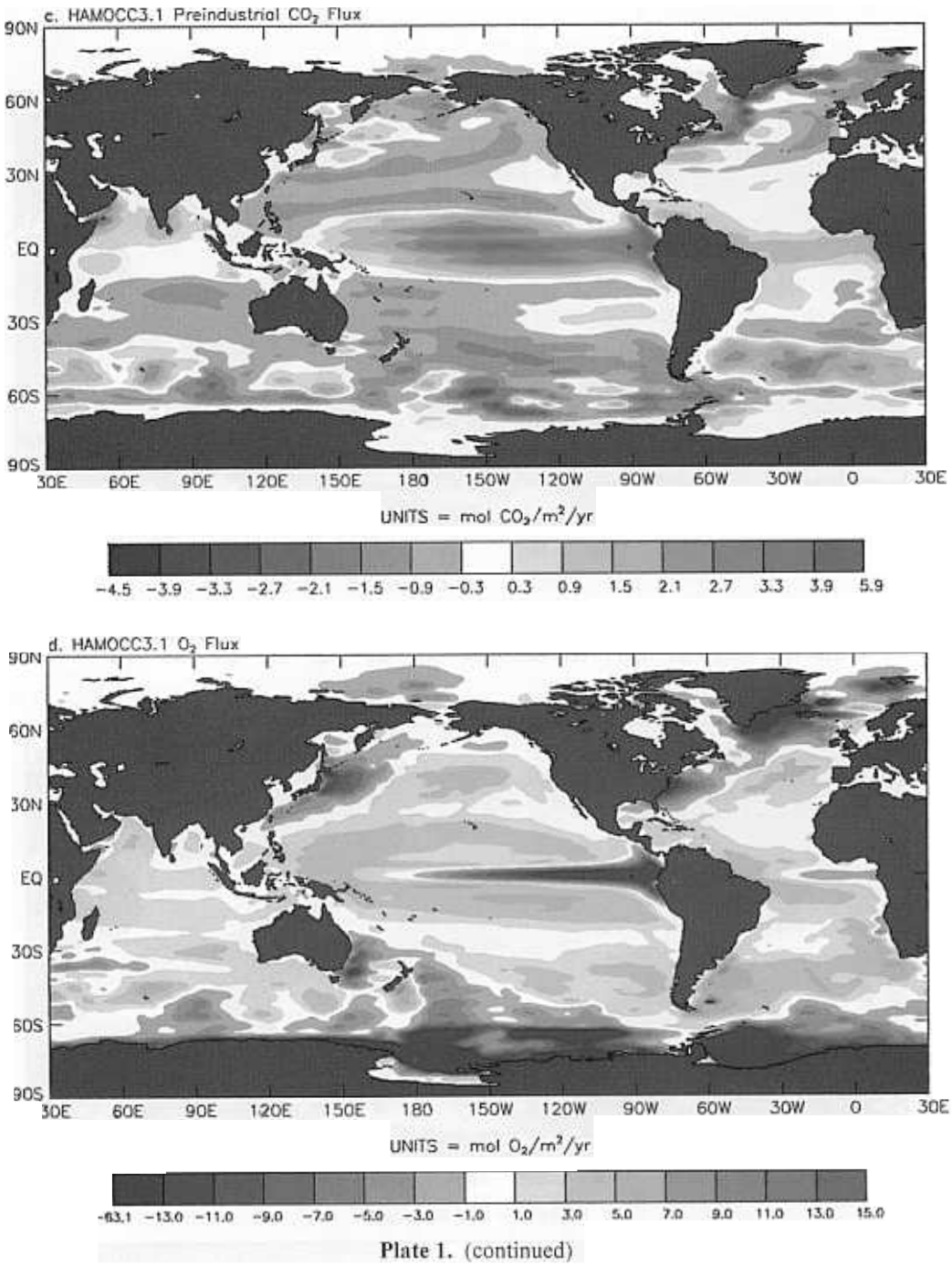

Plate 1. (continued)

ing the supply of DIC rich, O_2-depleted waters to the surface through model convection on the scale of a grid cell.

The physical fields for HAMOCC3.1 are taken from the large-scale geostrophic circulation model (LSG) [*Maier-Reimer et al.*, 1993]. This model has a horizontal resolution of 3.5° by 3.5° and 15 layers in the vertical and resolves the seasonal cycle on a 1-month time step. This model represents an improvement over earlier HAMOCC versions in that it includes a plankton model which allows nutrient uptake rates to vary seasonally thereby improving agreements with seasonal surface pCO_2 variations [*Six and Maier-Reimer*, 1996]. The model tracks PO_4, phytoplankton, zooplankton, POM, and DOC. New production in HAMOCC3.1 is parameterized by a Michaelis-Menton kinetics equation, based on simulated surface PO_4 concentrations and modified by light, temperature, vertical mixing, and phytoplankton abundance. The predicted latitudinal variations in annual-average PO_4 and O_2 saturation are generally in good agreement with observations.

Plate 1c shows the annual-average, preindustrial air-sea CO_2 fluxes predicted by HAMOCC3.1. The distribution of these fluxes is similar to that of the POBM CO_2 fluxes, with the exception of a slightly reduced CO_2 sink in the North

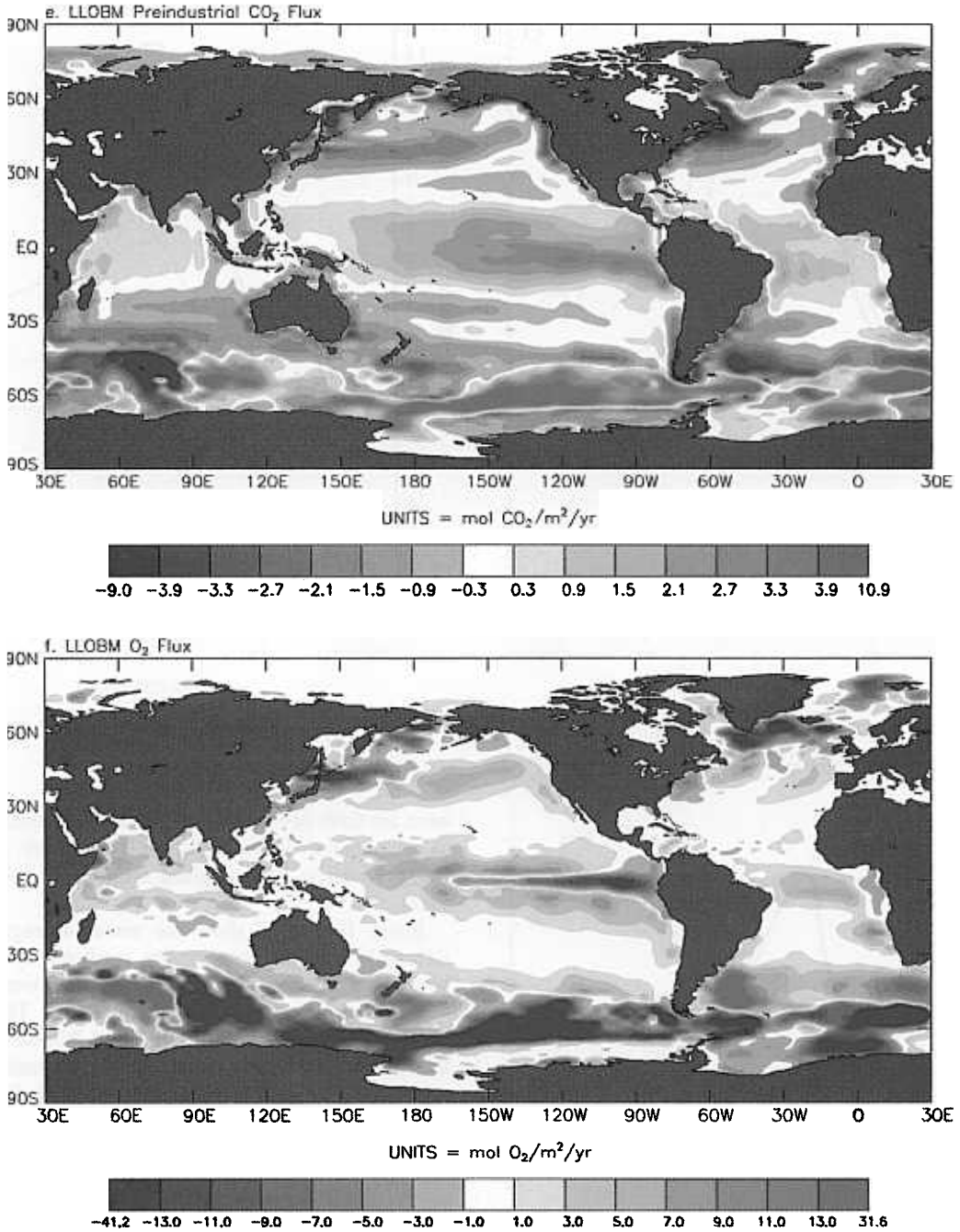

Plate 1. (continued)

Atlantic and a distinctly different pattern in the Southern Ocean. Plate 1d shows the annual-average O_2 flux predicted by HAMOCC3.1. This flux pattern is also similar to that of POBM, however, with a somewhat larger equatorial sink. In addition, HAMOCC3.1 predicts a very large O_2 sink in the Weddell Sea which is less strongly predicted by POBM. The HAMOCC3.1 heat fluxes indicate that this sink is primarily due to solubility forcing through the modeled convective formation of deep water.

The physical fields for LLOBM are based on a modified version of the GFDL model [*Duffy et al.*, 1997], which in the simulations used here had a resolution of 4° longitude by 2° latitude and 23 levels in the vertical. This model also has a similar biological parameterization to that of POBM. Productivity in LLOBM is simulated by forcing to seasonal PO_4 observations with a timescale of 2 weeks. Because it is known that this approach does not produce realistic seasonal variations in air-sea CO_2 and O_2 fluxes [*Six and Maier-Reimer*, 1996], we have only used the annual-average fluxes here. Of the new production in LLOBM, 80% is assumed to

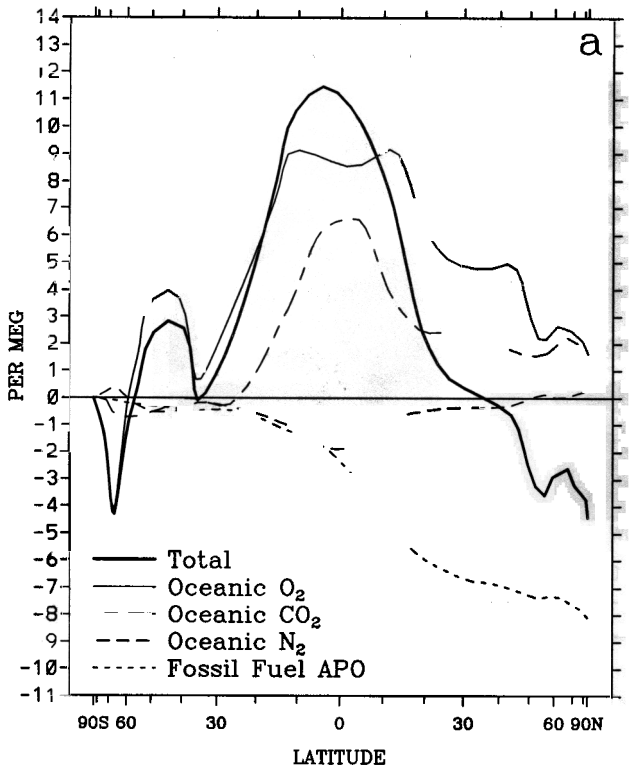

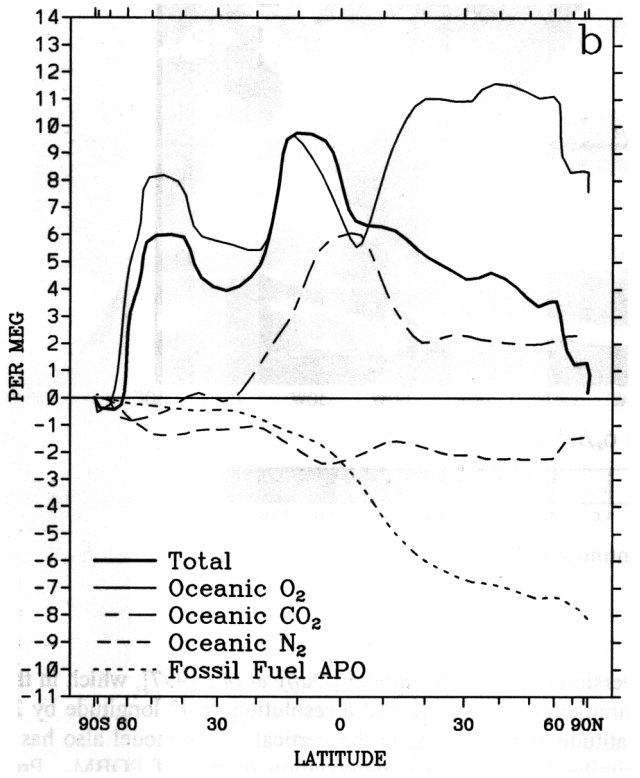

Figure 3. (a) The latitudinal APO variations as predicted by POBM-TM2 along the transect in Figure 1 and relative to the prediction at South Pole, along with the components. (b) Same as Figure 3a but as predicted by HAMOCC3.1-TM2. (c) Same as Figure 3a but as predicted by LLOBM-TM2.

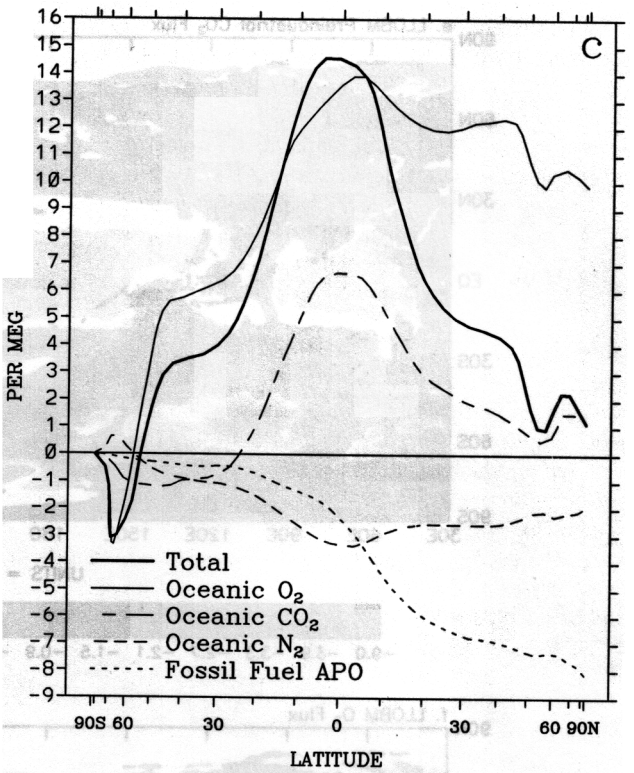

Figure 3. (continued)

be in the form of POM which sinks and is remineralized using an exponential depth scale, while the other 20% goes into DOM which is remineralized with a decay constant of 25 years.

Plates 1e and 1f show the annual-average, preindustrial CO_2 and O_2 fluxes, respectively, predicted by LLOBM. The large-scale patterns are similar to the other two models, again with the exception of the Southern Ocean. There are several similarities between the LLOBM and POBM fluxes, such as the CO_2 source/O_2 sink southwest of Australia and the CO_2 sink/O_2 source east of Argentina, which indicate that these two GFDL-based models are predicting grid-scale convection in many of the same regions. It is apparent from the molar magnitude of the fluxes shown in Plate 1 that the largest air-sea O_2 fluxes are an order of magnitude greater than the largest air-sea CO_2 fluxes. This is due to the reinforcing tendencies of the solubility and biological pumps as discussed above and to the more rapid gas exchange of O_2. When zonally integrated, however, the largest O_2 fluxes are only twice as large as the largest CO_2 fluxes; thus both significantly influence the meridional variations in APO.

5. Predicted Atmospheric Potential Oxygen Gradients

We used the preindustrial CO_2 (Plates 1a, 1c, and 1e), anthropogenic perturbation CO_2 (not shown), O_2 (Plates 1b, 1d, and 1f) , and N_2 (not shown) ocean model fluxes as lower boundary conditions in the TM2 atmospheric tracer transport

model [*Heimann*, 1995]. For the anthropogenic CO_2 flux, we used years 1990, 1987, and 1989 for POBM, HAMOCC3.1, and LLOBM, respectively. Only HAMOCC3.1 explicitly calculates air-sea N_2 fluxes. For POBM, we estimated the N_2 fluxes by scaling the solubility-driven O_2 fluxes according to the ratio of N_2 and O_2 solubilities. For LLOBM, we estimated N_2 fluxes based on solubility changes calculated from model heat fluxes. The TM2 model solves the tracer continuity equation using wind fields generated by the European Centre for Medium-Range Weather Forecasting analyses and a subgrid-scale vertical convection parameterization. In this study, we used analyzed winds from 1987. This model has a resolution of 8° latitude by 10° longitude with nine sigma layers in the vertical and a time step of 4 hours. The ocean model output fields were regridded onto the TM2 horizontal grid. We ran the model for 4 years, at which point the spatial concentration gradients are quasi-stationary, and used annual average values from the fourth year. Because the transport is linearly related to tracer concentration, various source components can be run separately, and the results can be combined for comparison to atmospheric observations.

Figure 3a shows the interhemispheric variation in APO and its components as predicted by POBM-TM2. The total curve is graphically the sum of the component curves and is calculated according to (5). The fossil fuel component is the same as that shown in Figure 2c. The oceanic components show greater structure than the fossil fuel component because of the proximity of the sources to the surface transect (Figure 1) used for the model predictions, while the oceanic O_2 component shows the most structure for the reasons discussed above. The oceanic CO_2 component reflects the strong equatorial outgassing shown in Plate 1a. Because of the greater ocean area in the southern hemisphere, the oceanic uptake of anthropogenic CO_2 leads to a decreasing CO_2 gradient to the south. The interhemispheric gradient in the O_2 component predicted by POBM-TM2 has an equatorial bulge with a small depression at the equator, which results from the combined biological and thermal effects also discussed above. The POBM-TM2 CO_2 and O_2 components combine to form a large equatorial peak in APO. The predicted APO structure in the southern hemisphere appears to result from the meridional separation of O_2 sources and sinks in the Southern Ocean as illustrated in Plate 1b. As Figure 3a shows, the thermally driven outgassing of N_2 near the equator leads to an apparent decrease in APO.

Figure 3b shows the interhemispheric variation in APO and its components as predicted by HAMOCC3.1-TM2. The fossil fuel component is identical, and the CO_2 and N_2 components are very similar to those predicted by POBM-TM2. The primary differences between the interhemispheric APO variations predicted by POBM-TM2 and HAMOCC3.1-TM2 are due to differences in the O_2 component. Most noticeably, the HAMOCC3.1-TM2 O_2 concentrations are lower around the equator and do not decrease as strongly toward the north. The equatorial O_2 depression seen in HAMOCC3.1-TM2 appears to be the result of both a stronger sink and seasonal covariations between air-sea O_2 fluxes and atmospheric mixing, as discussed below. Similar to POBM-TM2, HAMOCC3.1-TM2 predicts a small APO peak near 45°S with a significant decrease immediately to the south. This feature in HAMOCC3.1-TM2 also appears to be related to a pattern of O_2 sources in the northern half of the Southern Ocean and sinks in the southern half, including the strong sink in the Weddell Sea.

Figure 3c shows the interhemispheric variation in APO and its components as predicted by LLOBM-TM2. The shape of the total curve, with a large equatorial peak, is very similar to that of POBM-TM2. In the northern hemisphere, the LLOBM-TM2 O_2 component drops off less steeply than in POBM-TM2, indicating weaker O_2 sinks at high northern latitudes. However, the effect of this on APO is countered by the CO_2 component dropping off more steeply than in POBM-TM2, apparently because of stronger CO_2 sinks at high northern latitudes. In the southern hemisphere, the LLOBM-TM2 APO gradient has less structure than the other two models between 40° and 50°S but shows a similarly strong dip around 70°S.

6. Model/Observation Comparisons

Figure 4 shows the interhemispheric variation in APO as determined from atmospheric observations (from Figure 2c) and as predicted by POBM-TM2, HAMOCC3.1-TM2, and LLOBM-TM2 (from Figure 3). As described in section 3.3, variations in the observed APO values can only result from air-sea gas exchange and the relatively well-constrained fossil

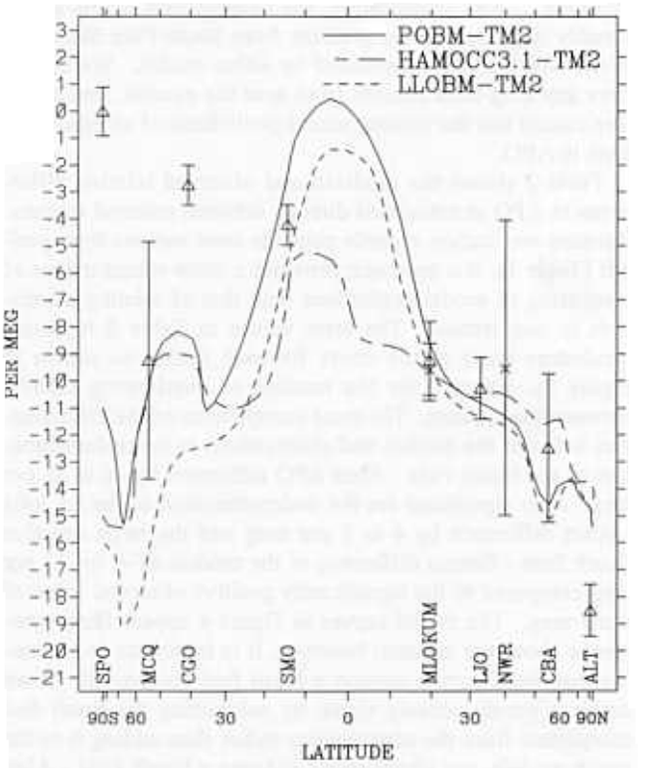

Figure 4. The observed latitudinal APO variations relative to South Pole (from Figure 2c) and the predictions of the three models (from Figure 3). The vertical scaling is the same as in Figure 3, but the model curves have been shifted to visually fit the northern midlatitude stations.

Table 2. Modeled and observed relative APO differences

Stations	POBM-TM2	HAMOCC3.1-TM2	LLOBM-TM2	Observed
CBA-ALT	0.1	2.1	0.0	4.6 ± 3.0
LJO-CBA	3.8	1.0	3.8	2.2 ± 3.5
KUM-LJO	2.2	1.0	1.7	1.0 ± 1.8
SMO-KUM	6.5	3.1	4.1	4.6 ± 1.5
CGO-SMO	-5.9	-2.2	-6.7	0.5 ± 1.2
MCQ-CGO	-2.1	-1.6	-4.0	-6.5 ± 4.3
SPO-MCQ	-0.7	-4.4	-0.3	10.8 ± 3.9
SPO-ALT	4.1	-0.9	-1.4	20.6 ± 1.4
LJO-ALT	4.0	3.1	3.8	8.2 ± 1.1
SPO-SMO	-8.6	-8.1	-11.0	4.2 ± 1.3

Values are per meg.

fuel effect. Thus the comparison in Figure 4 represents a direct test of the model predictions of the longitudinal variation of combined air-sea CO_2, O_2, and N_2 fluxes. While all three models produce reasonable fits to the observations between Samoa and Cold Bay, they disagree markedly outside of this region. None of the models produce the observed depression in APO at Alert, and all three of the models predict a decreasing gradient toward high southern latitudes which is not observed. Most significantly, the observations define a reasonably large decreasing gradient from South Pole Station to Alert, which is not reproduced by either model. We do not have any long-term records from near the equator, and therefore cannot test the various model predictions of an equatorial peak in APO.

Table 2 shows the modeled and observed relative differences in APO as calculated directly between selected stations. Because our station records coincide over various time periods (Table 1), this approach provides a more robust means of comparing to model predictions than that of relating all records to one station. The error values in Table 2 represent quadrature sums of the errors for each station as shown in Figure 2c, adjusted for the number of overlapping months between the stations. The most conspicuous of the discrepancies between the models and observations is the underestimation of the South Pole - Alert APO difference by 16 to 22 per meg. Also significant are the underestimation of the La Jolla - Alert difference by 4 to 5 per meg and the large negative South Pole - Samoa difference in the models of -8 to -11 per meg compared to the significantly positive observed value of 4 per meg. The model curves in Figure 4 appear fairly symmetric about the equator; however, it is important to remember that these curves contain a fossil fuel component. If we derive a purely oceanic signal by subtracting the fossil fuel component from the observations rather than adding it to the ocean models, our observations indicate a South Pole - Alert difference of around -13 per meg, while the models predict values between +3 and +9 per meg.

There are a number of possible explanations for these discrepancies. One possibility that we must consider, particularly when calculating relative differences between stations, is that of systematic biases in our sampling or measurement procedures. The TAC measurements shown in Figure 2a agree well with those of other sampling programs [*Keeling et al.*, 1989a, *Tans et al.*, 1990], and the $(O_2/N_2)_{corr}$ measurements shown in Figure 2b, though unique, reveal no unreasonable interstation differences. For APO, the comparison of the relatively proximal stations of Mauna Loa, Kumukahi, La Jolla, Niwot Ridge, and Cold Bay (see Figure 2c) suggests that systematic errors are similar to or smaller than our estimated precision. Observationally, the most difficult station is South Pole, where flasks must be stored for months at low ambient temperature and pressure. To date, we have found no systematic errors that could explain the discrepancy of around 12 per meg between the observed and modeled South Pole - Samoa APO difference [Keeling *et al.*, 1998a]. If the value of 1.1 for the O_2:CO_2 ratio of terrestrial photosynthesis and respiration were incorrect by more than the error estimates of *Severinghaus* [1995] or if this value varies systematically with latitude, our observed and modeled APO values would both change. However, the largest discrepancies we see are in the southern hemisphere where the terrestrial effects on APO are very small. Outside of the observations, the only other possible sources of error are the atmospheric transport model and the ocean models, which we now discuss in turn.

7. Atmospheric Transport Uncertainties

As *Law et al.* [1992] point out, atmospheric transport models may underestimate the meridional mixing efficiency at high southern latitudes by not accurately reproducing convective processes and transient disturbances in this region. While TM2 has been tested against Krypton 85 (^{85}Kr) and Radon 222 (^{222}Rn) and the model gives reasonable predictions of southern hemisphere meridional CO_2 gradients [*Heimann and Keeling*, 1989], none of these gases has strong southern hemisphere sources as O_2 does. However, as Figure 4 shows, enhanced meridional mixing in the southern hemisphere would only flatten the predicted gradients; it could not change their sign, which is necessary to bring them into agreement with the observations.

A transport problem that could potentially have a more significant effect on latitudinal APO gradients is the uncertainty in resolving the effects of seasonal covariations between surface fluxes and atmospheric mixing, known as rectifier effects. During summer at high latitudes, the marine boundary layer is stably stratified and the O_2 efflux due to surface warming and biological productivity is trapped near the surface, whereas during winter, strong vertical mixing in the atmosphere dilutes the surface O_2 deficit caused by cooling and deep ventilation. At low latitudes, seasonal variations in the Intertropical Convergence Zone cause the tropics to receive air preferentially from the winter hemisphere, where O_2 uptake is occurring. The net effect, as predicted by HAMOCC3.1-TM2 and shown in Figure 5, is that the purely seasonal O_2 flux component produces annual mean peaks of 1 to 2 per meg at the surface around 50° latitude in each hemisphere and a trough of 4 to 6 per meg at the surface within 20° of the equator. The relatively smaller equatorial APO bulge in HAMOCC3.1-TM2 compared to the other two models (Figure 4) may be partially explained by this effect.

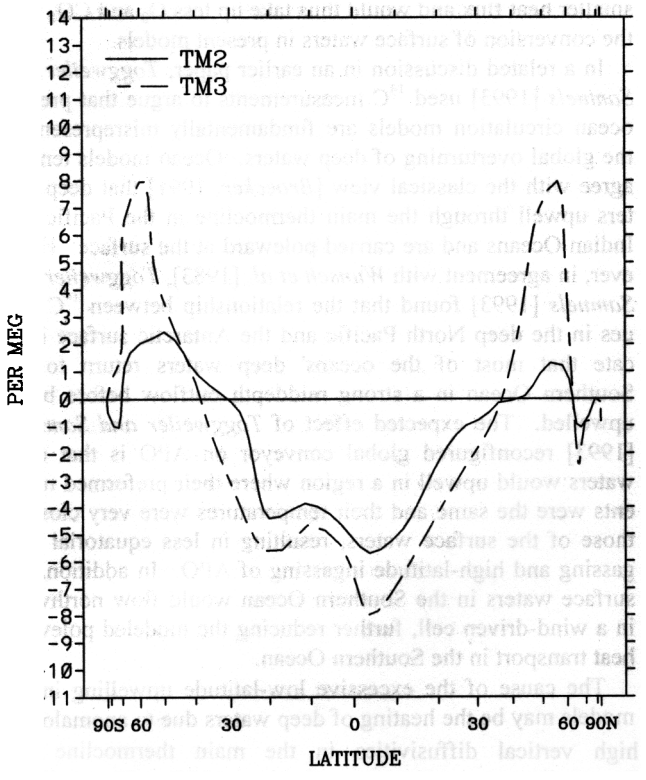

Figure 5. The latitudinal $\delta(O_2/N_2)_{corr}$ variations predicted by TM2 (solid curve) and TM3 (dashed curve) when driven by the purely seasonal component of the HAMOCC3.1 air-sea O_2 fluxes. The predictions are for the transect shown in Figure 1, where the TM3 values are taken from the second model level (approximately 170 m) to approximate selective sampling during well-mixed conditions. The vertical scaling is the same as for Figures 3 and 4.

To explore the uncertainty in the simulated rectifier effects, we ran the same sources on a 4° by 5° by 18-level version of the transport model (TM3) which produces significantly greater rectifier effects as shown in Figure 5. In the purely seasonal HAMOCC3.1-TM3 runs, the annual mean equatorial O_2 trough was slightly greater, while the peaks at 50° in each hemisphere were increased significantly to 8 per meg. This has the effect of bringing the HAMOCC3.1-TM3 Cold Bay - Alert APO difference (7.9 per meg) into agreement with the observations. However, this model also makes the La Jolla - Cold Bay prediction (-2.7 per meg) much worse. In addition, because the Cold Bay station is located inland, we do not expect its APO value to be as sensitive to marine boundary layer variations as TM3 predicts, and the improved agreement relative to Alert may be fortuitous. The HAMOCC3.1-TM3 predictions are also worse for the South Pole - Samoa difference (-12.5 per meg) and almost unchanged with respect to the most significant South Pole - Alert difference. While rectifier effects are clearly a large source of uncertainty in modeled latitudinal APO gradients, neither the TM2 nor the TM3 rectifier patterns can be scaled to consistently resolve the discrepancies shown here.

8. Ocean Model Uncertainties

The similarity among the model predictions in Figure 4 suggests that if the discrepancies with observations are due to the ocean models, the problems are likely fundamental to all three models. One aspect of coarse-resolution ocean models that has received considerable attention is that of the parameterization of subgrid-scale isopycnal eddy mixing [*Veronis*, 1975; *Gent and McWilliams*, 1990; *Duffy et al.*, 1997]. The three models tested here all simulate this process through horizontal diffusion. However, as pointed out by *Veronis* [1975], in regions of steeply sloping isopycnals this method can lead to artificial water, heat, and tracer transports. The feature consisting of a peak in APO around 45°S and a trough to the south (Figure 4), may be a result of such artificial transport in the Deacon cell, a meridional cell which appears in the zonally averaged mean velocity field as downwelling around 45°S and upwelling around 60°S [*Döös and Webb*, 1994]. In models which employ horizontal diffusion, advective transport in this cell results in a moderate air-to-sea heat flux at 45°S and a very strong sea-to-air heat flux at 60°S. By parameterizing the dynamical effect of subgrid-scale eddies through the diffusion of tracers and isopycnal thicknesses along isopycnals [*Gent and McWilliams*, 1990], *Danabasoglu et al.* [1994] showed that transport of heat and tracers by these eddies almost completely cancels the advective transport in the Deacon cell. Their model also produced less convec-

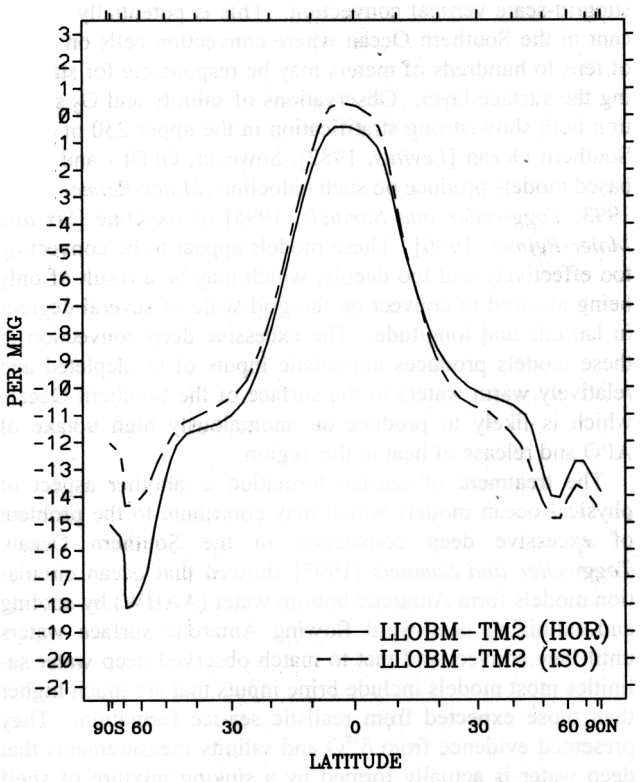

Figure 6. The latitudinal APO variations predicted by two versions of LLOBM-TM2, using horizontal diffusion (solid curve) (from Figure 3c) and using the parameterization of Gent and McWilliams [1990] (dashed curve). The vertical scaling is the same as for Figures 3-5.

tion in the Southern Ocean and a confinement of the region of deep water formation in the North Atlantic.

These results, as they pertain to the meridional overturning of dissolved O_2, DIC, and heat, have potentially significant implications for model predictions of air-sea APO flux. The parameterization of *Gent and McWilliams* [1990] has been shown to significantly improve some ocean model simulations [*Boning et al.*, 1995; *McDougall et al.*, 1996], but also to worsen others [*Duffy et al.*, 1997]. To investigate the sensitivity of modeled APO variations to this parameterization, we have used output from a version of LLOBM which incorporated the *Gent and McWilliams* [1990] mixing scheme. Figure 6 shows a comparison between the meridional APO gradients predicted by this version of LLOBM-TM2 and the previous version (Figure 3c) which used horizontal diffusion. Incorporating the *Gent and McWilliams* [1990] scheme produced a decrease in APO in the northern hemisphere and an increase and flattening of APO in the southern hemisphere. As Figures 4 and 6 show, these changes are of the right sense to bring the predicted APO variations into better agreement with the observations; however, the magnitude of change is much too small. While this suggests that the *Gent and McWilliams* [1990] parameterization cannot resolve the large discrepancy with observations, it does not rule out the possibility that isopycnal eddy mixing is a large source of model error or that including this parameterization in other models might produce a more significant change.

Another limitation of POBM, HAMOCC3.1, and LLOBM related to their coarse resolution is that they do not simulate subgrid-scale vertical convection. This is potentially significant in the Southern Ocean where convection cells on scales of tens to hundreds of meters may be responsible for stabilizing the surface layer. Observations of salinity and O_2 saturation both show strong stratification in the upper 250 m of the Southern Ocean [*Levitus*, 1982]; however, GFDL- and LSG-based models produce no such halocline [*Maier-Reimer et al.*, 1993; *Toggweiler and Samuels*, 1995] or oxycline [*Six and Maier-Reimer*, 1996]. These models appear to be convecting too effectively and too deeply, which may be a result of only being allowed to convect on the grid scale of several degrees in latitude and longitude. The excessive deep convection in these models produces unrealistic inputs of O_2-depleted and relatively warm waters to the surface of the Southern Ocean, which is likely to produce an anomalously high uptake of APO and release of heat in this region.

The treatment of sea-ice formation is another aspect of physical ocean models which may contribute to the problem of excessive deep convection in the Southern Ocean. *Toggweiler and Samuels* [1995] showed that ocean circulation models form Antarctic bottom water (AABW) by cooling and salinizing southward flowing Antarctic surface waters until they convect and that to match observed deep water salinities most models include brine inputs that are much higher than those expected from realistic sea-ice formation. They presented evidence from $\delta^{18}O$ and salinity measurements that deep water is actually formed by a sinking mixture of shelf water and southward flowing circumpolar deep water (CDW), which requires much smaller brine inputs to match observed deep salinities. The implication of this result for APO predictions is that converting CDW into AABW requires a much smaller heat flux and would thus take up less O_2 and CO_2 than the conversion of surface waters in present models.

In a related discussion in an earlier paper, *Toggweiler and Samuels* [1993] used ^{14}C measurements to argue that present ocean circulation models are fundamentally misrepresenting the global overturning of deep waters. Ocean models tend to agree with the classical view [*Broecker*, 1991] that deep waters upwell through the main thermocline in the Pacific and Indian Oceans and are carried poleward at the surface. However, in agreement with *Wunsch et al.* [1983], *Toggweiler and Samuels* [1993] found that the relationship between ^{14}C values in the deep North Pacific and the Antarctic surface indicate that most of the oceans' deep waters return to the Southern Ocean in a strong middepth outflow before being upwelled. The expected effect of *Toggweiler and Samuels'* [1993] reconfigured global conveyor on APO is that deep waters would upwell in a region where their preformed nutrients were the same and their temperatures were very close to those of the surface waters, resulting in less equatorial outgassing and high-latitude ingassing of APO. In addition, the surface waters in the Southern Ocean would flow northward in a wind-driven cell, further reducing the modeled poleward heat transport in the Southern Ocean.

The cause of the excessive low-latitude upwelling in the models may be the heating of deep waters due to anomalously high vertical diffusivities in the main thermocline (R. Toggweiler, personal communication, 1997). These diffusivities are currently set as low as numerical considerations will allow; however, they may still overestimate mixing. To get a model to produce realistic middepth outflows, Toggweiler et al. (manuscript submitted to *Journal of Geophysical Research*, 1997) found they needed to artificially cool the deep ocean south of the Antarctic Circumpolar Current so that advective heat loss to the south could replace low-latitude upwelling as the dominant heat sink for the deep Pacific and Indian Oceans. While this improves the pattern of the flow, it results in even higher sea-to-air heat fluxes near Antarctica. This excessive throughput of heat by the abyssal ocean may continue to be a source of uncertainty in APO simulations until its apparent cause, low-latitude inputs of heat from excessive vertical mixing, is resolved.

Improvements in any of the just described model deficiencies, lack of subgrid-scale eddies, lack of subgrid-scale vertical convection, too high salt inputs to Southern Ocean, and too high vertical diffusivities in the main thermocline, all have the potential to reduce the heat flux out of the Southern Ocean and the poleward transport of heat by the southern hemisphere oceans. These changes are in the right sense to bring the model predictions into agreement with the observations (Figure 4), and as previously mentioned, we expect APO to be particularly sensitive to heat flux-driven solubility changes. *Toggweiler and Samuels* [1995] point out that sea-to-air heat fluxes in the Weddell and Ross Seas predicted by GFDL- and LSG-based models can be twice as large as indicated by observations. Whether the result shown in Figure 4 is symptomatic of solely a problem with the physical ocean models or not, efforts to improve the models' representation of heat fluxes are needed to improve their chemical flux predictions.

While potential problems in the physical ocean models fit

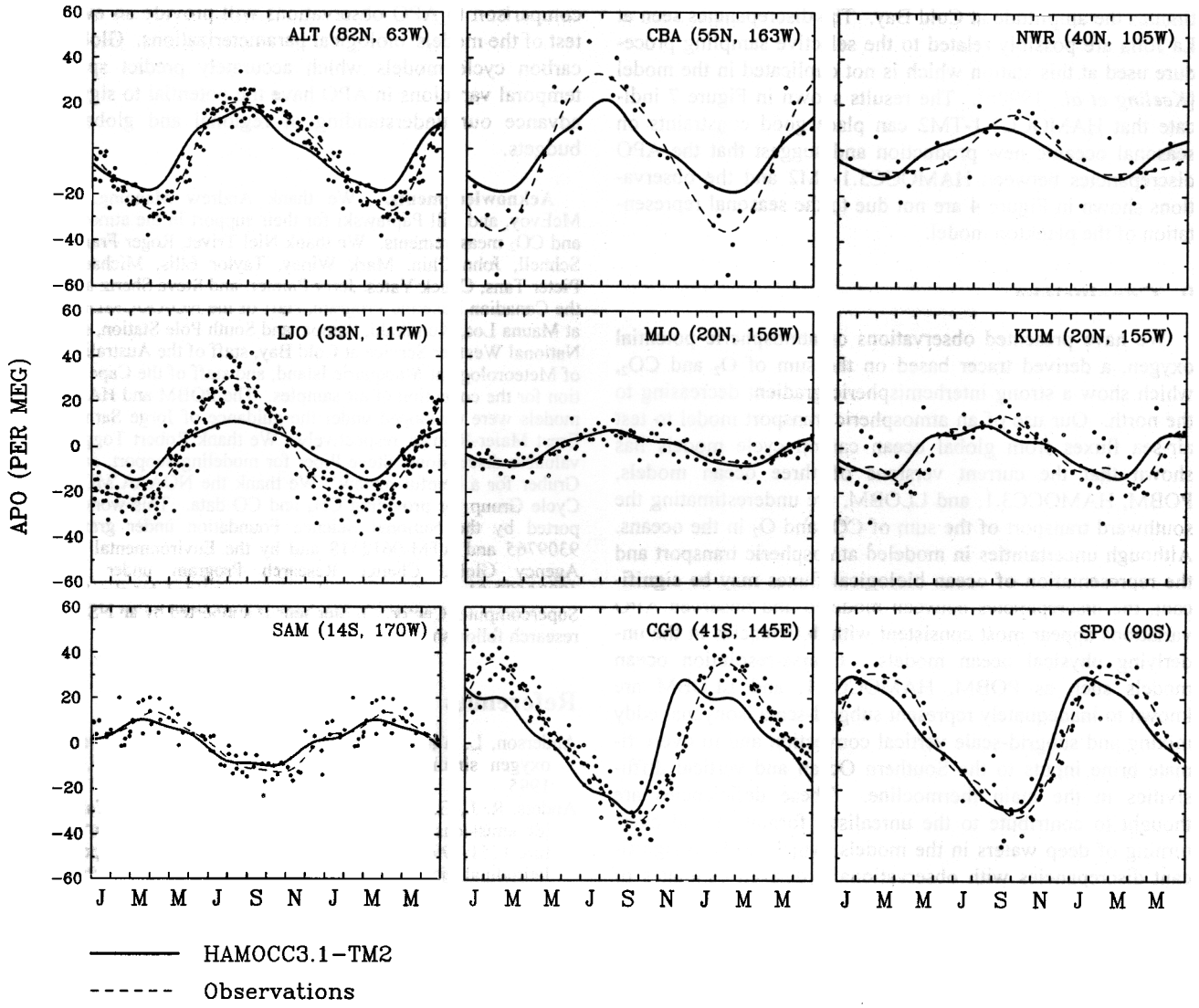

Figure 7. Seasonal variations in APO observed and predicted by HAMOCC3.1-TM2 for all of the stations except Macquarie Island. Observations from several years are plotted in one climatological year and have not been corrected for CO and CH_4. Lines are four-harmonic fits to the observations and HAMOCC3.1-TM2 predictions, except at Cold Bay and Niwot Ridge, where two-harmonic fits are used.

with the observed discrepancies, the biological parameterizations themselves may also contribute to the disagreement. In the case of HAMOCC3.1, basing the calculation of primary productivity on one nutrient, PO_4, may lead to an overestimation of production in high-nutrient, low-chlorophyll regions where other nutrients have a limiting effect. In the case of the POBM and LLOBM parameterizations, if the model-predicted regions of upwelling are spatially offset from those in the real ocean, forcing model PO_4 concentrations to agree with local observations will lead to spurious production in these regions. Also, *Six and Maier-Reimer* [1996] have shown that the inclusion of a plankton model in HAMOCC3.1, which the tested versions of POBM and LLOBM are without, significantly altered the distribution of export production. Misrepresentation of hemispheric biological biases, such as enhanced iron fertilization in the northern hemisphere, could also lead to errors in the predicted meridional CO_2 and O_2 variations (Weber et al., manuscript in preparation, 1998). However, because of the counteracting effect of biological CO_2 and O_2 fluxes on APO, errors in the biological components of these models are less likely to produce the large discrepancies seen in Figure 4.

We can further test HAMOCC3.1 by comparing the predicted seasonal variations in APO to those observed at our stations. Figure 7 shows this comparison for all of the stations except Macquarie Island. As Figure 7 shows, the combined HAMOCC3.1-TM2 model does a remarkably good job of reproducing the phase and amplitudes of the observed cycles. Figure 7 confirms the favorable O_2/N_2 comparison at Cape Grim presented by *Six and Maier-Reimer* [1996]. The model predicts a slightly advanced phase at Alert, Niwot Ridge, Kumukahi, Cape Grim, and South Pole, and underes-

timates the amplitude at Cold Bay. The discrepancies seen at La Jolla are possibly related to the selective sampling procedure used at this station which is not duplicated in the model [*Keeling et al.*, 1998b]. The results shown in Figure 7 indicate that HAMOCC3.1-TM2 can place good constraints on seasonal oceanic new production and suggest that the APO discrepancies between HAMOCC3.1-TM2 and the observations shown in Figure 4 are not due to the seasonal representation of the plankton model.

9. Conclusions

We have presented observations of atmospheric potential oxygen, a derived tracer based on the sum of O_2 and CO_2, which show a strong interhemispheric gradient decreasing to the north. Our use of an atmospheric transport model to test air-sea fluxes from global ocean carbon cycle models has shown that the current versions of three ocean models, POBM, HAMOCC3.1, and LLOBM, are underestimating the southward transport of the sum of CO_2 and O_2 in the oceans. Although uncertainties in modeled atmospheric transport and the representation of ocean biological fluxes may be significant, the discrepancies between modeled and observed APO variations appear most consistent with deficiencies in the underlying physical ocean models. Coarse-resolution ocean models such as POBM, HAMOCC3.1, and LLOBM are known to inadequately represent subgrid-scale isopycnal eddy mixing and subgrid-scale vertical convection and to overestimate brine inputs to the Southern Ocean and vertical diffusivities in the main thermocline. These deficiencies are thought to contribute to the unrealistic formation and overturning of deep waters in the models, which leads to significant discrepancies with observationally derived estimates of ocean heat transport.

The large disagreement shown in Figure 4 may be less surprising when one considers that climate simulations, using similar ocean models coupled to atmospheric global climate models, have required significant air-sea energy flux adjustments to maintain a realistic model state [*Manabe et al.*, 1991]. In this study, we have coupled ocean and atmosphere models chemically and appear to require analogous chemical flux adjustments to reproduce the observed state. The excessive uptake of APO by the Southern Ocean and too low uptake in the far Northern Oceans indicated in Figure 4 has implications for estimates of regional uptake of anthropogenic CO_2. Our results are consistent with those of *Gruber et al.* [1998], who found that POBM significantly overestimates the observed inventory of anthropogenic CO_2 south of 50°S. A decrease in the Southern Ocean CO_2 uptake would also improve agreements with atmospheric CO_2 observations which indicate a CO_2 source in this region [*Tans et al.*, 1990].

Efforts are currently underway to improve simulations of large-scale ocean circulation and deep water formation and their effect on heat and tracer transports. Future comparisons to APO will benefit from the extension of our current O_2 measurement records and the addition of O_2 measurements targeting sensitive regions. Especially helpful would be additional stations south of 40°S, across the Equatorial Pacific, and closer to the North Atlantic region. If uncertainties in the physical components of the ocean models can be reduced, the comparison to APO observations will provide an even better test of the models' biological parameterizations. Global ocean carbon cycle models which accurately predict spatial and temporal variations in APO have the potential to significantly advance our understanding of regional and global carbon budgets.

Acknowledgments. We thank Andrew Manning, Elizabeth McEvoy, and Bill Paplawski for their support in the atmospheric O_2 and CO_2 measurements. We thank Niel Trivet, Roger Francey, Russ Schnell, John Chin, Mark Winey, Taylor Ellis, Michael Bender, Pieter Tans, Chuck Yates, Jerry Painter, and Steve Shertz and staff at the Canadian Baseline Program, staff of the NOAA/CMDL program at Mauna Loa, Kumikahi, Samoa, and South Pole Station, staff of the National Weather Service at Cold Bay, staff of the Australian Bureau of Meteorology at Macquarie Island, and staff of the Cape Grim Station for the collection of air samples. The POBM and HAMOCC3.1 models were developed under the guidance of Jorge Sarmiento and Ernst Maier-Reimer, respectively. We thank Robert Toggweiler for valuable discussions, Steve Piper for modeling support, and Nicolas Gruber for a helpful review. We thank the NOAA/CMDL Carbon Cycle Group for providing CH_4 and CO data. This work was supported by the National Science Foundation under grants ATM-9309765 and ATM-9612518 and by the Environmental Protection Agency Global Change Research Program under IAG#DW-49935603-01-2. Computer time was provided by the San Diego Supercomputer Center. B. Stephens is supported by an NSF graduate research fellowship.

References

Anderson, L. A., and J. L. Sarmiento, Global ocean phosphate and oxygen simulations, *Global Biogeochem. Cycles, 9,* 621-636, 1995.

Andres, R. J., G. Marland, T. Boden, and S. Bischoff, Carbon dioxide emissions from fossil fuel combustion and cement manufacture 1751-1991 and an estimate of their isotopic composition and latitudinal distribution, in *1993 Global Change Institute*, edited by T. Wigley and D. Schimel, in press, Cambridge Univ. Press, New York, 1998.

Bacastow, R., and E. Maier-Reimer, Dissolved organic carbon in modeling oceanic new production, *Global Biogeochem. Cycles, 5,* 71-85, 1991.

Boning, C. W., W. R. Holland, F. O. Bryan, G. Danabasoglu, and J. C. McWilliams, An overlooked problem in model simulations of the thermohaline circulation and heat transport in the Atlantic Ocean, *J. Clim., 8,* 515-523, 1995.

Brewer, P. G., C. Goyet, and D. Dyrssen, Carbon dioxide transport by ocean currents at 25° N latitude in the Atlantic Ocean, *Science, 246,* 477-479, 1989.

Broecker, W. S., The great global conveyor, *Oceanography, 2,* 79-89, 1991.

Broecker, W. S., and T.-H. Peng, Interhemispheric transport of carbon dioxide by ocean circulation, *Nature, 356,* 587-589, 1992.

Danabasoglu, G., J. C. McWilliams, and P. R. Gent, The role of mesoscale tracer transports in the global ocean circulation, *Science, 264,* 1123-1126, 1994.

Dlugokencky, E. J., P. M. Lang, K. A. Masarie and L. P. Steele, Atmospheric CH_4 records from sites in the NOAA/CMDL air sampling network, in *Trends '93: A Compendium of Data on Global Change,* edited by T. A. Boden, et al., *ORNL/CDIAC Rep. 65,* pp. 274-350, Carbon Dioxide Inf. Anal. Cent., Oak Ridge Nat. Lab., Oak Ridge, Tenn., 1994.

Döös, K., and D. J. Webb, The Deacon cell and the other meridional cells of the Southern Ocean, *J. Phys. Oceanogr., 24,* 429-442, 1994.

Duffy, P. B., K. Caldeira, J. Selvaggi, and M. I. Hoffert, Effects of subgrid-scale mixing parameterizations on simulated distributions of natural ^{14}C, temperature, and salinity in a three-dimensional ocean general circulation model, *J. Phys. Oceanogr., 27,* 498-523, 1997.

Enting, I. G., and J. V. Mansbridge, Seasonal sources and sinks of atmospheric CO_2: Direct inversion of filtered data, *Tellus, Ser. B, 41*, 111-126, 1989.

Enting, I. G., C. M. Trudinger, and R. J. Francey, A synthesis inversion of the concentration and $\delta^{13}C$ of atmospheric CO_2, *Tellus, Ser. B, 47*, 35-52, 1995.

Erickson, D. J., P. J. Rasch, P. P. Tans, P. Friedlingstein, P. Ciais, E. Maier-Reimer, K. Six, C. A. Fischer, and S. Walters, The seasonal cycle of atmospheric CO_2: A study based on the NCAR Community Climate Model (CCM2), *J. Geophys. Res., 101*, 15079-15097, 1996.

Gent, P. R., and J. C. McWilliams, Isopycnal mixing in ocean circulation models, *J. Phys. Oceanogr., 20*, 150-155, 1990.

Gruber, N., J. L. Sarmiento, and T. F. Stocker, An improved method for detecting anthropogenic CO_2 in the oceans, *Global Biogeochem. Cycles, 10*, 809-837, 1996.

Gruber, N., Anthropogenic CO_2 in the Atlantic Ocean, Global Biogeochem. Cycles, in press, 1998.

Heimann, M., The global atmospheric tracer model TM2, *Tech. Rep. 10*, 53 pp., Dtsch. Klimarechenzentrum, Hamburg, Germany, 1995.

Heimann, M., and C. D. Keeling, A three-dimensional model of atmospheric CO_2 transport based on observed winds, 2, Model description and simulated tracer experiments, in *Aspects of Climate Variability in the Pacific and Western Americas, Geophys. Monogr. Ser.*, vol. 55, edited by D. H. Peterson, pp. 237-275, AGU, Washington D. C., 1989.

Heimann, M., and E. Maier-Reimer, On the relations between the oceanic uptake of CO_2 and its carbon isotopes, *Global Biogeochem. Cycles, 10*, 89-110, 1996.

Keeling, C. D., R. B. Bacastow, A. F. Carter, S. C. Piper, T. P. Whorf, M. Heimann, W. G. Mook, and H. Roeloffzen, A three-dimensional model of atmospheric CO_2 transport based on observed winds, 1, Analysis of observational data, in *Aspects of Climate Variability in the Pacific and Western Americas, Geophys. Monogr. Ser.*, vol. 55, edited by D. H. Peterson, pp. 165-236, AGU, Washington D. C., 1989a.

Keeling, C. D., S. C. Piper, and M. Heimann, A three-dimensional model of atmospheric CO_2 transport based on observed winds, 4, Mean annual gradients and interannual variations, in *Aspects of Climate Variability in the Pacific and Western Americas, Geophys. Monogr. Ser.*, vol. 55, edited by D. H. Peterson, pp. 305-363, AGU, Washington D. C., 1989b.

Keeling, R. F., Development of an interferometric oxygen analyzer for precise measurement of the atmospheric O_2 mole fraction, Ph.D. thesis, 178 pp., Harvard Univ., Cambridge, Mass., 1988.

Keeling, R. F., and T.-H. Peng, Transport of heat, CO_2 and O_2 by the Atlantic's thermohaline circulation, *Philos. Trans. R. Soc. London Ser. B, 348*, 133-142, 1995.

Keeling, R. F., and S. R. Shertz, Seasonal and interannual variations in atmospheric oxygen and implications for the global carbon cycle, *Nature, 358*, 723-727, 1992.

Keeling, R. F., R. G. Najjar, M. L. Bender, and P. P. Tans, What atmospheric oxygen measurements can tell us about the global carbon cycle, *Global Biogeochem. Cycles, 7*, 37-67, 1993.

Keeling, R. F., S. C. Piper, and M. Heimann, Global and hemispheric CO_2 sinks deduced from changes in atmospheric O_2 concentration, *Nature, 381*, 218-221, 1996.

Keeling, R. F., A. C. Manning, E. M. McEvoy, S. R. Shertz, Methods for measuring changes in atmospheric O_2 concentration and their application in southern hemisphere air, *J. Geophys. Res.*, in press, 1998a.

Keeling, R. F., B. B. Stephens, R. G. Najjar, S. C. Doney, D. Archer, and M. Heimann, Seasonal variations in the atmospheric O_2/N_2 ratio in relation to the air-sea exchange of O_2, *Global Biogeochem. Cycles*, in press, 1998b.

Law, R. M., I. Simmonds, and W. F. Budd, Application of an atmospheric tracer model to high southern latitudes, *Tellus Ser. B, 44*, 358-370, 1992.

Levitus, S., Climatological atlas of the world ocean, *NOAA Prof. Pap. 13*, 173 pp., U.S. Dep. of Comm., Washington, D. C., 1982.

Maier-Reimer, E., Geochemical cycles in an ocean general circulation model: Preindustrial tracer distributions, *Global Biogeochem. Cycles, 7*, 645-677, 1993.

Maier-Reimer, E., U. Mikolajewicz, and K. Hasselmann, Mean circulation of the Hamburg LSG OGCM and its sensitivity to the thermohaline surface forcing, *J. Phys. Oceanogr., 23*, 731-757, 1993.

Maier-Reimer, E., U. Mikolajewicz, and A. Winguth, Future ocean uptake of CO_2: Interaction between ocean circulation and biology, *Clim. Dyn., 12*, 711-721, 1996.

Manabe, S., R. J. Stouffer, M. J. Spelman, and K. Bryan, Transient response of a coupled ocean-atmosphere model to gradual changes of atmospheric CO_2, I, Annual mean response, *J. Clim., 4*, 785-818, 1991.

Marland, G., R. M. Rotty, and N. L. Treat, CO_2 from fossil fuel burning: Global distribution of emissions, *Tellus Ser. B, 37*, 243-258, 1985.

McDougall, T. J., A. C. Hirst, M. H. England, and P. C. McIntosh, Implications of a new eddy parameterization for ocean models, *Geophys. Res. Lett., 23*, 2085-2088, 1996.

Najjar, R.G., Simulations of the phosphorous and oxygen cycles in the world ocean using a general circulation model, Ph.D. thesis, 190 pp., Princeton Univ., Princeton, N. J., 1990.

Najjar, R. G., J. L. Sarmiento, and J. R. Toggweiler, Downward transport and the fate of organic matter in the ocean: Simulations with a general circulation model, *Global Biogeochem. Cycles, 6*, 45-76, 1992.

Novelli, P. C., L. P. Steele, and P. P. Tans, Mixing ratios of carbon monoxide in the troposphere, *J. Geophys. Res., 97*, 20731-20750, 1992.

Sarmiento, J. L., and C. Le Quéré, Oceanic carbon dioxide uptake in a model of century-scale global warming, *Science, 274*, 1346-1350, 1996.

Sarmiento, J. L., J. R. Toggweiler, and R. Najjar, Ocean carbon-cycle dynamics and atmospheric pCO_2, *Philos. Trans. R. Soc. London Ser. A, 325*, 3-21, 1988.

Sarmiento, J. L., R. D. Slater, M. J. R. Fasham, H. W. Ducklow, J. R. Toggweiler, and G. T. Evans, A seasonal three-dimensional ecosystem model of nitrogen cycling in the North Atlantic euphotic zone, *Global Biogeochem. Cycles, 7*, 417-450, 1993.

Sarmiento, J. L., R. Murnane and C. Le Quéré, Air-sea CO_2 transfer and the carbon budget of the North Atlantic, *Philos. Trans. R. Soc. London Ser. B, 348*, 211-219, 1995.

Severinghaus, J. P., Studies of the terrestrial O_2 and carbon cycles in sand dune gases and in Biosphere 2, Ph.D. thesis, 148 pp., Columbia Univ., New York, 1995.

Six, K., and E. Maier-Reimer, Effects of plankton dynamics on carbon fluxes in an ocean general circulation model, *Global Biogeochem. Cycles, 10*, 559-583, 1996.

Takahashi, T., T. T. Takahashi, and S. C. Sutherland, An assessment of the role of the North Atlantic as a CO_2 sink, *Philos. Trans. R. Soc. London Ser. B, 348*, 143-152, 1995.

Tans, P. P., I. Y. Fung, and T. Takahashi, Observational constraints on the atmospheric CO_2 budget, *Science, 247*, 1431-1438, 1990.

Toggweiler, J. R., and B. Samuels, New radiocarbon constraints on the upwelling of abyssal water to the ocean's surface, in *The Global Carbon Cycle*, edited by M. Heimann, *NATO ASI Ser.*, vol. I 15, pp. 333-336, 1993.

Toggweiler, J. R., and B. Samuels, Effect of sea ice on the salinity of Antarctic bottom waters, *J. Phys. Oceanogr., 25*, 1980-1997, 1995.

Toggweiler, J. R., K. Dixon, and K. Bryan, Simulations of radiocarbon in a coarse-resolution world ocean model, 1, Steady state prebomb distributions, *J. Geophys. Res., 94*, 8217-8242, 1989a.

Toggweiler, J. R., K. Dixon, and K. Bryan, Simulations of radiocarbon in a coarse-resolution world ocean model, 2, Distribution of bomb-produced carbon 14, *J. Geophys. Res., 94*, 8243-8264, 1989b.

Veronis, G., The role of models in tracer studies, in *Numerical Models of the Ocean Circulations*, pp. 133-146, Natl. Acad. of Sci., Washington, D. C., 1975.

Volk, T., and M. I. Hoffert, Ocean carbon pumps: Analysis of relative strengths and efficiencies in ocean-driven atmospheric CO_2 changes, in *The Carbon Cycle and Atmospheric CO_2: Natural Variations Archean to Present, Geophys. Monogr. Ser.*, vol. 32, edited by E. T. Sundquist and W. S. Broecker, pp. 99-110, AGU, Washington D. C., 1985.

Wunsch C., D. X. Hu, and B. Grant, Mass, heat, salt, and nutrient fluxes in the South Pacific Ocean, *J. Phys. Oceanogr., 13*, 725-753, 1983.

K. Caldeira, Lawrence Livermore National Laboratory, Livermore, CA 94550. (e-mail: kenc@LLNL.gov)

M. Heimann and K.D. Six, Max Planck Institut für Meteorologie, 20146 Hamburg, Germany. (e-mail: martin.heimann@dkrz.de; six@dkrz.de)

R.F. Keeling and B.B. Stephens, Scripps Institution of Oceanography, University of California, San Diego, La Jolla, CA 92093. (e-mail: rkeeling@ucsd.edu; britt@ucsd.edu)

R. Murnane, Bermuda Biological Station for Research, Inc., Ferry Reach, GE01, St. George's, Bermuda. (e-mail: rmurnane@bbsr.edu)

(Received May 17, 1997; revised November 10, 1997; accepted November 24, 1997.)